Kinematic Effects and the B Meson*

AUSTIN M. GLEESON
Physics Department, Syracuse University, Syracuse, New York
(Received 23 February 1967)

Two mechanisms for the enhancement of threshold resonances are described. These mechanisms are applied to the case of the B meson.

IN this paper, a brief discussion of the kinematical basis of the B meson is presented. In a recent paper,[1] it was proposed that a peak in the $\pi+\pi\to\pi+\omega$ spectrum could be generated by the addition of energy dependence in the resonance width of the ρ meson. In that paper, a numerical calculation of a model is used to fit the data and the detail operation of the model is obscured. Here we propose to study two mechanisms which could lead to the presence of a kinematical enhancement at the B meson. Both mechanisms are intimately related to the application of unitarity to multichannel scattering processes and, therefore, the unitarity constraints must be observed at all points in the discussion.

A qualitative test of these mechanisms can be made in any of several possible models, but the simplest approach is to modify slightly the model of Ref. 1. The model is developed from the multichannel N/D expression for the scattering of a $J^P=1^-$, $T=1$ meson system. The three channels of interest are $\pi+\pi$ (1), $\pi+\omega$ (2), and $\eta+\rho$ (3).

An amplitude f_{ij} related to the t_{ij} of the scattering amplitude is defined by

$$f_{ij}=\{g_i\}^{1/2}t_{ij}\{g_j\}^{1/2},$$

where the g_i's are the factors required to remove the kinematical singularities in t_{ij}.[2] The g_i's will also reproduce the threshold behavior. It should be noted that the g_i's can be modified with a suitable entire function and still satisfy the requirements for the kinematic singularities. In this model, the g_i's are chosen to be asymptotically bounded. In Ref. 1, the g_i's are not so chosen and this affects the behavior of the amplitude in a nontrivial way. This problem will be discussed in the context of the model as developed in later sections. The f_{ij} satisfy the usual unitarity modified by the required kinematical factors.

The model is driven by a fixed left-hand pole. The $\mathbf{f}$ matrix becomes

$$f_{ij}=\frac{\tilde{C}_i\tilde{C}_j}{s-s_P}[1-R_1(s)\tilde{C}_1^2-R_2(s)\tilde{C}_2^2-R_3(s)\tilde{C}_3^2]^{-1},$$

where i, $j=1$, 2, 3 designates the channels as labeled above. This decoupled form is a general result for all multichannel N/D with a single fixed pole. The functions $R_i(s)$ are the usual phase-space factors with allowance for the kinematical effects,

$$R_i(s)=\frac{(s-s_P)}{\pi}\int_{t_i}^{\infty}\frac{\rho_i(s')ds'}{(s'-s_P)^2(s'-s-i\epsilon)}.$$

The phase-space and coupling factors are

$$\rho_i(s)=\tfrac{1}{8}|\mathbf{p}_i/\sqrt{s}|^3,\quad \tilde{C}_i^2=g^0{}_{\rho i}{}^2/4\pi,$$

and t_i is the ith threshold. (Note: $\tilde{C}$ has the dimensions of mass.) Imposing an effective-range approximation in the denominator, forcing the appearance of the ρ meson, and renormalizing the couplings, the cross section is found to have the form

$$\sigma_{ij}=\frac{12\pi}{p_i^2}\frac{\Gamma_i(s)\Gamma_j(s)}{(s-m_\rho)^2+[\sum_i\Gamma_i(s)]^2},$$

where $\Gamma_i(s)=\rho_i(s)C_i^2\theta(s-t_i)$ and $C_i^2=g_{\rho i}{}^2/4\pi$.

This relatively simple equation for the multichannel cross section will be the basis for the conclusions that follow. An immediate observation is that any approximation which holds the Γ's in the denominator constant violates unitarity. The neglect of variation of the kinematic factors would require that the Γ's in the numerator and denominator be held constant together. Another observation that is essential for the development of this paper is the bounds implied by unitarity. The unitarity bounds are established by setting the real part of the amplitude to zero. The effective unitarity bounds of the model are then

$$\sigma_{ij}(s)\leq\sigma_{ij}{}^{(B)}(s)\equiv\frac{12\pi}{p_i^2}\frac{\Gamma_i(s)\Gamma_j(s)}{[\sum_k\Gamma_k(s)]^2}.$$

In this model with ReD replaced by a linear function and the ρ-resonance fit as a zero of ReD, then equality is obtained only as $s=m_\rho$.

$$\sigma_{ij}(m_\rho)=\sigma_{ij}{}^{(B)}(m_\rho).$$

More detailed models would be characterized by more complex behavior of the real part of the D, ImD which controls the unitarity bounds would be of the same general nature. It is possible to produce a model with fixed Γ with unitarity which produces an effect which could be interpreted as a resonance. It is also in the

* Work supported in part by the U. S. Atomic Energy Commission.
[1] M. Parkinson, Phys. Rev. Letters **18**, 270 (1967).
[2] J. Franklin, Phys. Rev. **152**, 1437 (1966); G. Frye and R. L. Warnock, *ibid.* **130**, 478 (1963).

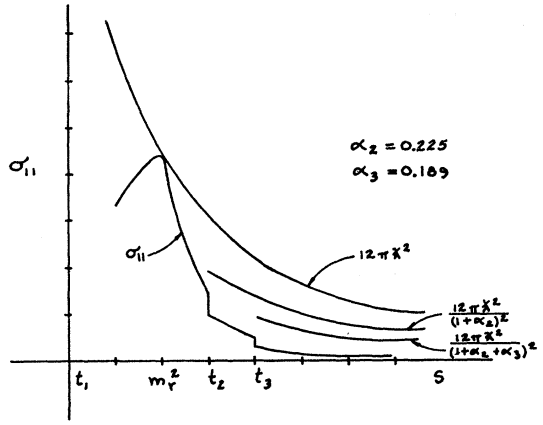

FIG. 1. Effective unitarity limits for σ_{11} for weak cross-coupling case.

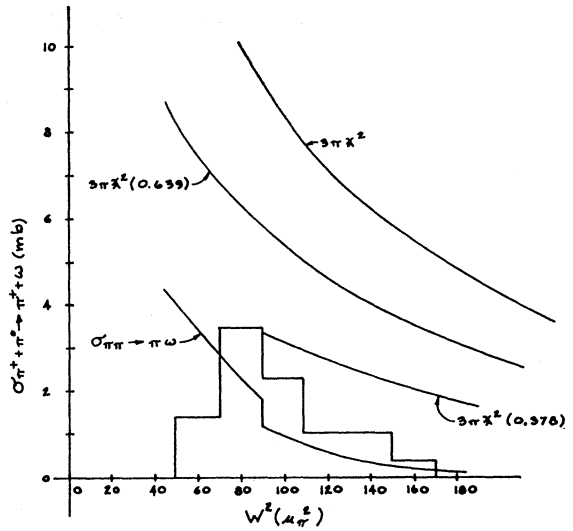

FIG. 3. Plot of experimental data versus simple ρ–resonance model.

context of this model that the other mechanism of enhancement can most clearly be displayed. This second mechanism is responsible for the behavior of the cross section in Ref. 1.

The model describes two situations with three channels with fixed entrance widths $\Gamma_i=\alpha_i\Gamma_1$. The first situation is shown in Figs. 1 and 2, and is characterized as the weakly cross-coupled case. In this case $\alpha_2<1$, and $\alpha_3\approx\alpha_2$. The diagrams show the effective unitarity limits of the cross section. The parameters are $\Gamma_1=m_\rho^2$ $-t_1=t_2-t_3$ and $\alpha_2=0.225$, $\alpha_3=0.189$. For the strong cross coupling, the same widths and thresholds apply, but $\alpha_2=4.455$ and $\alpha_3=1.245$. This choice allows the exact same curve for σ_{12} in both the strong and the weak cross-coupling limit. For the strong cross coupling, the σ_{11} curve is virtually zero above t_2. The physical basis for this behavior is obvious. In the weak-coupling case the beam divides between σ_{11} and σ_{12} and σ_{22}, with σ_{22} small and σ_{11} large. The σ_{11} feeds the inelastic channel. In the strong-coupling situation, the roles of σ_{11} and σ_{22} are reversed from those above. The important feature of σ_{12} in this model is the pronounced peak in σ_{12} just before t_3. The associated σ_{11} curve does not have nearly as pronounced an effect and the enhancement is restricted to the production channel. This is the first of the two mechanisms associated with unitarity which enhance only the production cross section. This first mechanism is effective in both the strong- and the weak-coupling limits. In Fig. 3, the experimental data[3] are compared with the effective unitarity plots of $\sigma(\pi+\pi\to\pi+\omega)$. We observe that the opening of the $\rho+\eta$ channel produces a peak in the unitarity bounds of the $\pi+\omega$ channel. The parameters used to derive the figure are taken from the latest $SU(3)$ values. We used $\alpha_2=4$ and $\alpha_3=4\sin^2\theta$, where θ is the $\omega-\varphi$ mixing angle, $\theta\approx38°$. We also plot the cross section using only the ρ resonance as a driving force. It is satisfying that the ρ resonance does not saturate the data. As expected, the neglect of the kinematic factors implies that the amplitude does not rise off of threshold as required.

The second mechanism to be discussed is relevant to the strong-coupling case only and requires the presence of the kinematic factors. It does not require the presence of the third channel. This mechanism is based on the behavior of the effective unitarity limit when α_2 is varied. Note that the kinematic factors are normally

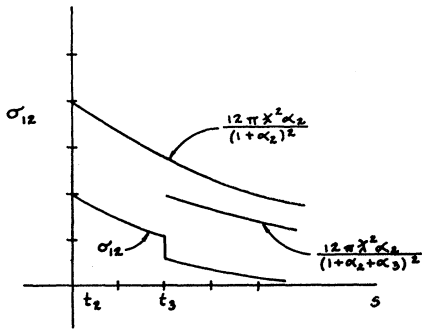

FIG. 2. Effective unitarity limits for σ_{12} for weak and strong cross coupling.

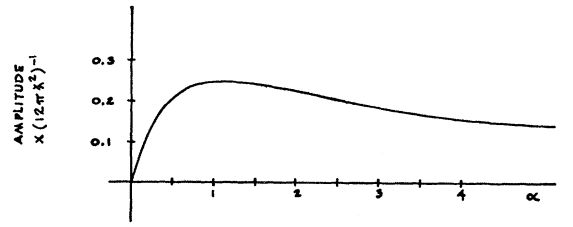

FIG. 4. Plot of limits of effective unitarity as a function of α_2, the relative channel width.

[3] N. Xuong, R. L. Lander, W. A. W. Mehlhop, and P. M. Yager, Phys. Rev. Letters **11**, 227 (1963).

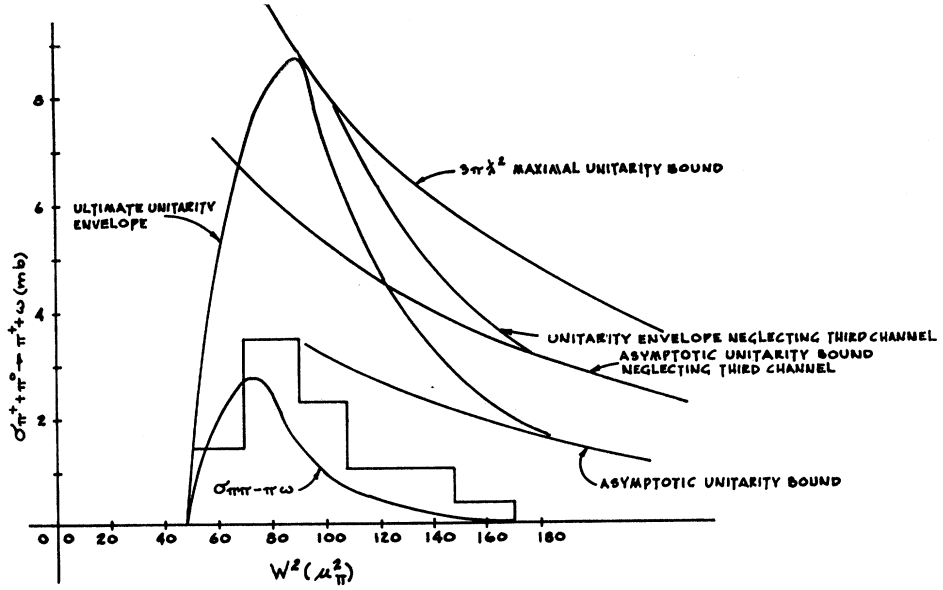

FIG. 5. Plot of unitarity envelopes with momentum-dependent entrance widths.

added to compensate for the poor threshold behavior of a constant-half-width cross section. In this model with threshold dependence built into the channel widths, the parameter α_2 is now given by

$$\alpha_2=(|\mathbf{p}_2|/|\mathbf{p}_1|)^3 g^2{}_{\rho 2}/g_{\rho 1}{}^2.$$

In Fig. 4, the effective unitarity limit as a function of α_2 is plotted. The mechanism by which a threshold bump can be enhanced is now apparent. In Fig. 4 at $\alpha_2=1$, the effective unitarity bound of the inelastic channel achieves a maximum. As the energy increases above the threshold, the kinematic factors force α_2 to vary from zero to its asymptotic value $g_{\rho 2}{}^2/g_{\rho 1}{}^2$. In the weak cross-coupled case ($g_{\rho 2}{}^2/g_{\rho 1}{}^2<1$) nothing interesting happens. The kinematic factors merely force the correct threshold dependence upon the production cross section. In the strong cross-coupled case ($g_{\rho 2}{}^2/g_{\rho 1}{}^2>1$) a new effect arises. The kinematic factors now cause α_2 to rise from zero, introducing the correct threshold dependence. As the energy increases, the α_2 will go through unity and maximize the effective unitarity bound at $3\pi\lambda^2$. Further increases in energy cause the effective unitarity bound to decrease to the lower value associated with the asymptotic value of α_2. This enhancement of the unitarity envelope reflects itself in the production cross section. In Fig. 5, this effect is applied to the case of the B meson. Here the strong cross coupling is applicable and the unitarity envelope reaches for its maximum value but then returns to its normal value as the kinematic factors go to unitarity. In the diagram there are several curves. First the effective unitarity envelopes of Fig. 3 are shown. Then the effect of the kinematic factors which would be present with no $\rho+\eta$ channel added. The inner envelope is the resultant unitarity bound with all factors included. Finally, the production cross section for the model with the resonance driving is shown. Again, although it reproduces the general shape, this model produces a cross section somewhat too small to explain all the data.

In Ref. 1, a model very similar to the one presented here produced a cross section too strong for the data. There are two fundamental reasons for this behavior. First, the model of Ref. 1 omitted the presence of the $\rho+\eta$ channel. The second and more striking reason, alluded to earlier, is the presence of nonbounded kinematic factors. The choice of what type of entire function can be used to modify the kinematic factors is generally quite arbitrary. In this case, the use of nonbounded kinematic factors would lead to an excellent fit to the experimental data. The basic reason for this effect is that at large energy the imaginary part of the amplitude dominates the real part and the cross section tends asymptotically to the unitarity limits. In ρ-meson-driven models, this effect sets in fairly quickly and of course causes the amplitude to trail off too slowly. There are several reasons why this model has been constructed with bounded kinematic factors. The ρ meson is certainly not the only force present and is not expected to saturate the data. The use of nonbounded kinematic factors raises the question of subtractions in the N/D formalism.

There are several other competing channels whose effects have been omitted in this model. These channels are found to have a small effect in the $\sigma(\pi^+ + \pi^0 \to \pi^+ + \omega)$ cross section. The $K\bar{K}$ channel has too low a threshold to sharply effect the B peak, and its couplings are weaker than the strong cross coupling required here. The $\pi+\varphi$ channel has zero entrance width. The $N\bar{N}$ channel is too massive to be of real interest.

This model has shown how unitarity can impose

kinematic enhancements on the cross section of production processes. These enhancements, although present in the elastic channels, are quite marked in the production channel. The first mechanism for producing these enhancements is the opening of a new channel slightly behind the production threshold. The principal criterion for the effectiveness of this mechanism is the strength of the new channel relative to the original channels. A second mechanism is more novel and arises only in the strong cross-coupling case. This second mechanism is also dependent on the presence of kinematic factors depend on p^{2l+1}, the higher the l of the channel, the more effective this second mechanism will be. Both mechanisms are applied to the case of the B meson and produce the desired result. In this case, the low l restricts the effect of the second mechanim.

PHYSICAL REVIEW VOLUME 161, NUMBER 5 25 SEPTEMBER 1967

Relationship for the Vector-Meson–Lepton–Neutrino Coupling Constant

P. DU T. VAN DER MERWE*
Atomic Energy Board, Pelindaba, Republic of South Africa
(Received 13 April 1967)

A relationship is derived for the weak coupling constant of the vector-meson–lepton–neutrino vertex employing the notion of a conserved vector $SU(3)$ current and assuming a pole-dominance model. In the $SU(3)$ limit, a certain restriction on the Cabibbo angle results so that the theory contains no free parameters. Utilizing these results, the decay rates for $\rho \to l+\nu$ and $K^* \to l+\nu$ are calculated.

I. INTRODUCTION

IN this paper the $SU(3)$ theory of the two-body leptonic decays of vector mesons is considered. The main result of the investigation is the derivation of a relationship for the coupling constant γ of the vector-meson–lepton–neutrino vertex which in the $SU(3)$ limit reads

$$\gamma=(G/f)M^2{}_V. \tag{1}$$

In the last expression, G denotes the Fermi coupling constant, f the strong $(\rho\pi\pi)$ coupling constant, and M_V the mass of the vector meson.

This result is reminiscent of the Goldberger-Treiman relation[1] in terms of which the pion leptonic decay is explained to about 10%. The derivation of Eq. (1) is based on the notion of a conserved vector $SU(3)$ current[2] and an assumption of a pole-dominance model analogous to the Nambu derivation[3] of the Goldberger-Treiman relation. These results are presented in Sec. II.

In Sec. III, Eq. (1) is utilized to calculate the $\rho \to l+\nu$ and $K^* \to l+\nu$ decay rates.

II. THE COUPLING CONSTANT

In the $SU(3)$ theory, the Lagrangian density responsible for the two-body leptonic decays of vector mesons is given by

$$L=\gamma \,\mathrm{Tr}[v_\lambda C_V]\bar{u}_l(p)\gamma_\lambda(1-i\gamma_5)u_\nu(q), \tag{2}$$

where

$$v_\lambda=\begin{bmatrix} \left(\frac{1}{\sqrt{6}}\phi+\frac{1}{\sqrt{2}}\rho^0\right) & \rho^+ & K^{*+} \\ \rho^- & \left(\frac{1}{\sqrt{6}}\phi-\frac{1}{\sqrt{2}}\rho^0\right) & K^{*0} \\ K^{*-} & \bar{K}^{*0} & -(\sqrt{\tfrac{2}{3}})\phi \end{bmatrix} \tag{3}$$

and

$$C_V=\begin{bmatrix} 0 & \cos\theta_V & \sin\theta_V \\ 0 & 0 & 0 \\ 0 & 0 & 0 \end{bmatrix}, \tag{4}$$

which embodies the selection rules of weak interactions.[2]

The main interest of this paper consists in the derivation of a relationship for the coupling constant γ in terms of known quantities.

To this end we consider the three-body leptonic processes depicted in Fig. 1.

In a previous paper[2] we discussed a treatment of the three-body leptonic decays of mesons based on the

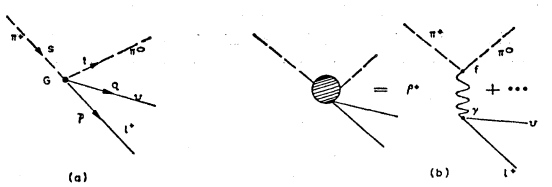

FIG. 1. Pion leptonic decay (a) in the current-current theory; and (b) in a pole dominance model.

* Address for correspondence: Atomic Energy Board, Private Bag 256, Pretoria, South Africa.

[1] M. L. Goldberger and S. B. Treiman, Phys. Rev. **111**, 354 (1958).

[2] P. du T. van der Merwe (unpublished).

[3] Y. Nambu, Phys. Rev. Letters **4**, 380 (1960); M. Gell-Mann and M. Lévy, Nuovo Cimento **16**, 705 (1960).